OBSERVED SEASONAL WEATHER REGIMES: IMPACT ON WIND SPEED AND TEMPERATURE

BSC-ESS-2016

Nicola Cortesi, Nube González-Reviriego,
Albert Soret and Francisco J. Doblas-Reyes

Earth Sciences Department
Barcelona Supercomputing Center - Centro Nacional de Supercomputación (BSC-CNS)

04 April 2017

TECHNICAL REPORT

Series: Earth Sciences (ES) Technical Report

A full list of ES Publications can be found on our website under:

https://earth.bsc.es/wiki/doku.php?id=library:external:technical_memoranda

Summary

Identifying the characteristics of the observed main modes of variability over Europe is a necessary step before comparing them with the modes simulated by models. This document describes the seasonal evolution of the European weather regimes, one of the more commonly employed classification of the modes of variability in the Northern Atlantic-European region. They were defined by means of a clustering analysis performed at seasonal time scale. The observational uncertainty in their patterns, interannual variability, trends and impact on wind speed and temperature was estimated comparing two different reanalysis (ERA-Interim and JRA-55). Results suggest that the frequency of the weather regimes did not change significantly in last 30 years and that their influence on wind speed and temperature can be high not only in winter, as already documented in the literature, but also during the other seasons. This is especially the case of offshore areas in the Mediterranean Sea, Baltic Sea and the Atlantic Ocean.

Contents

Index of figures

1. Introduction

The detection of the main modes of variability of the atmosphere requires classifying the continuum of all the possible states of the atmospheric circulation in a discrete number of recurrent and quasi-stationary patterns. It is the main approach employed in synoptic climatology to investigate extra-tropical atmospheric variability (Cassou et al., 2004). Since atmospheric trajectories tend to reside in preferred regions of the phase space, the complex atmospheric dynamics can be described by analyzing the frequency of occurrence and the persistence of a few patterns (Ferranti et al., 2015).

The aim of this study is to detect and characterize the main modes of variability of the sea level pressure (SLP) and their frequencies over Europe at seasonal time scale together with their impact on wind speed and temperature. Both analyses have been undertaken by using two different reanalysis datasets. The atmospheric circulation variability was classified by performing clustering algorithms on daily SLP anomalies over the North Atlantic-European region, to obtain the so-called weather regimes (WRs). WRs are also employed in the literature as synonymous of weather types. However, WRs are typically larger in scale, fewer in number, and persist longer than the weather types (Neal et al., 2016). The number of WRs depends on the study and the spatial domain. For the North Atlantic-European region, the more commonly used approach is based on the Bayesian information selection criteria (BIC) and defines four WRs: "NAO+" regime, "NAO-" regime, "Blocking" regime and "Atlantic Ridge" regime (Yiou & Nogaj, 2004). The "NAO+" and "NAO-" regimes are highly correlated with the positive and the negative phase of the North Atlantic Oscillation (NAO). In fact, NAO is most strongly felt the North Atlantic-European region (Trigo et al., 2004). The "Blocking" regime is associated with local reversals of the mid-latitude westerlies (Barriopedro et al., 2006), with stable high pressure patterns over Europe. The "Atlantic Ridge" regime is characterized by a strong anticyclonic ridge over the Atlantic Ocean (Cassou et al., 2004).

WRs are traditionally obtained using cluster analysis or classification methods. More complex approaches such as artificial neural network have also been proposed (Johnson et al., 2008). Most studies on WRs in the northern hemisphere focus on the winter season (Fil & Dubus, 2005, Michelangeli et al., 1995), or the whole cold season from October to April (Ferranti et al., 2015). This is because in these months WRs are more stable in time (more persistent) and have a stronger influence on local climate. Between the studies that classify four WRs over the North Atlantic-European region by clustering of a circulation variable, Cassou et al. (2004) employs SLP data from NCEP reanalysis during DJF (1950-2001). A subsequent work of the same author (Cassou et al., 2005) also focuses on the summer season but relying on Z500 anomalies and filtering them with a PCA before clustering. The same methodology applied to Z500 is also followed by Cattiaux et al. (2013) and is used to assess the reproducibility of WRs in a global model. Similarly, Ferranti et al. (2015) and Neal et al. (2016) use the weather regime paradigm to verify weather forecast systems. Yiou & Nogaj (2004) apply a classification method similar to Cassou et al. (2005), but for DJF period. Finally, Vrac et al. (2014) utilize the WRs to redefine the very concept of seasonality.

Between the more relevant impact studies of the WRs in the scientific literature, Salameh et al. (2009) employ the approach of Cassou et al. (2004) to study the impact of WRs on wind speed and wind direction in the southern part of France. Hurrell & Deser (2009) employ the same approach to study the links between the WRs and the NAO index. Couto et al. (2015) investigate the impact of WRs on the wind power in Portugal. Cassou (2006) evaluates the impact of WRs during the 2003 heat wave. All the above-mentioned works apply the k-means clustering method described firstly by Michelangeli et al. (1995).

To the best of our knowledge, only winter and summer WRs have been analyzed for the European region in the literature, mainly because due to their relatively homogeneous circulation behavior. Thus, results for both spring and autumn WRs and their impacts on wind speed and temperature are presented here for the first time.

This study is organized as follows. Section 2 describes the approach employed for the classification of the WRs and how such a classification was employed to generate the results presented in Section 3. Section 3 is divided in three parts: the first one compares the results for the two reanalysis, the second one describes the impact of the WRs on wind speed and the third one describes the impact of the WRs on temperature. Finally, Section 4 confronts this study with similar ones and draws some conclusions.

2. Data and methodology

2.1. Data

We used daily-means data of SLP, 10-m wind speed and 2-m mean temperature from two different reanalysis data sets: ERA-Interim (Dee et al., 2011) and JRA-55 (Kobayashi et al. 2015), with a spatial resolution of 0.75° and 1.25°, respectively. Daily-mean data were computed as an average of 6-hourly raw data (00, 06, 12 and 18 UTC). Daily SLP were employed for classifying the WRs, while daily wind speed and temperature were used to measure the impact of the WRs on these two variables, since these are the two variables object of study. This study, in fact, was done in the framework of the CLIM4ENERGY project inside the Copernicus Climate Change Service initiative and as part of the objectives of the RESILIENCE project funded by the Spanish Ministry of Economy. The daily means of the SLP were considered in this project, because the atmosphere tends to persist in the same WR for 5-7 days before evolving to a different regime (Fil & Dubus, 2005). SLP data is noisier than 500-hPa geopotential height (Z500), but, on the other hand, the SLP time series have the advantage of not showing any temporal trend (Hafez & Almazroui, 2014), so it was preferred to Z500. In the present study, we selected all the variables for the North Atlantic-European region (27°N–81°N, 85.5°W–45°E) for the period 1979-2013. For each individual season (DJF, MAM, JJA, SON), we obtained the daily anomalies taking the seasonal climatology for the same period as reference.

2.2. Methodology

Several variants of the WRs classification exist in the scientific literature. Nevertheless, here we adopted the approach followed by Météo-France with the aim of defining a standard basis for the comparison of the results. The comparison will be beneficial given the current scarcity of information in the literature on the impact of WRs on climate, especially for seasons different from winter and for climate variables different from temperature.

Most of the studies available in the literature perform a principal component analysis (PCA or EOFs) before classifying the WRs. However, the PCA filtering was not applied in this project in order to also take into account the more extreme SLP values, which are usually filtered out by the PCA process. Here, a classification of WRs was performed with the non-linear k-means cluster algorithm of Hartingan & Wong (with 30 random starts and a maximum of 100 iterations) applied for each season to the daily SLP anomalies. The classification depends on the region and the season selected. In case of the North Atlantic-European region, four WRs were selected for each season, accordingly to the BIC optimization criteria (Vrac et al., 2014). A summary of the different steps followed to obtain the WRs classification is illustrated in a flux diagram (Figure 1).

The clustering classification is created after splitting the data in seasons and converting the daily-mean data to daily anomalies based on the seasonal climatology (i.e: the average daily SLP of all days in period 1979-2013). The four possible values of the daily time series obtained from the k-means clustering corresponds to the four WRs (as the clustering assigns each daily

SLP anomaly pattern to one cluster only). From this classification, the SLP pattern associated to a given WR (hereafter WR pattern) and its interannual frequency were obtained. The seasonal WR pattern consists of the average of the SLP anomalies of all days associated with a given WR and season. The frequency of a WR refers to the time series of the seasonal frequencies of the given WR from 1979 to 2013 (see Figure 1). Frequencies are shown as the percentage of all days in the season associated to a given WR, and they are plotted in red/blue bars if their value is respectively higher/lower than the climatological frequency over the period 1979-2013. A Mann-Kendall test was introduced to identify significant trends in the frequency time series. If the trend is significant at the 95% confidence level, a black line is drawn over the frequency time series.

Once the daily time series of the four WRs is obtained, the impact of a WR on wind speed (or temperature) can be measured by averaging the 10-m wind speed (or 2-m temperature) anomalies of all days associated to the given WR and season. Impact maps were calculated only for the European region, because the main interest in this project is to measure the impact over land and the surrounding sea shore, and not in the middle of the ocean. A t-test was performed to assess the level of significance of the anomalies. Figure 1 illustrates schematically the sequence of steps involved in the measurement of the impact maps.

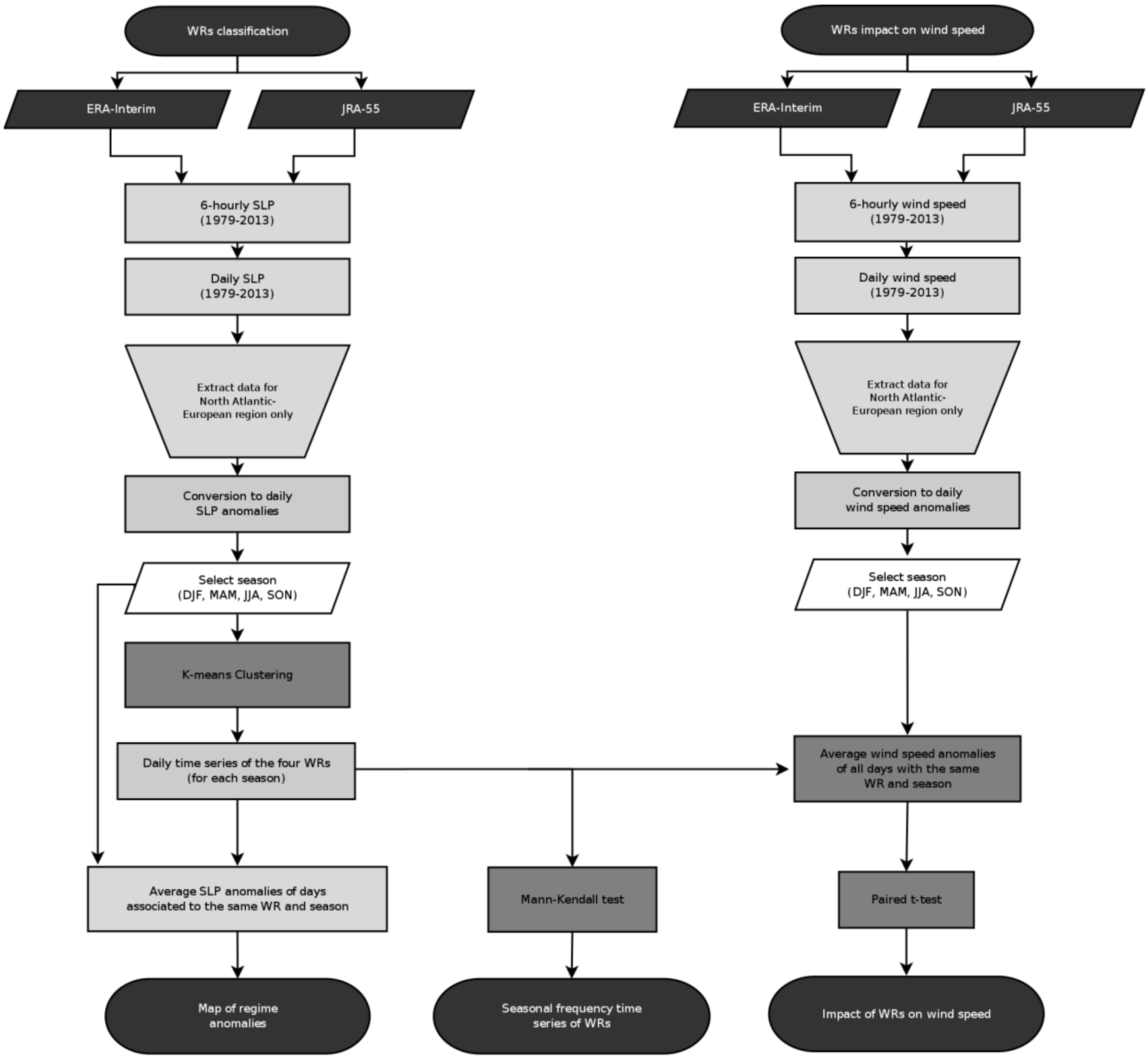

***Figure 1**. Flow chart of the WRs classification and of the impact analysis*

Flow chart with the sequence of the steps followed to obtain the classification of the weather regimes and the WRs impact on wind speed, starting from raw data up to the extraction of the WRs patterns and frequencies. A similar sequence was adopted for the impact of the WRs on temperature.

3. Results

3.1. Regime comparison between ERA-Interim and JRA-55

Even though the two reanalyses employed have different spatial resolutions (0.75° for ERA-Interim and 1.25° for JRA-55), the WR patterns measured from both datasets are almost identical all over the North Atlantic-European region for all seasons. For example, in Figure 2a and b a comparison between the two reanalysis is shown for the NAO+ regime in winter. SLP positive and negative anomalies are centered over the same areas and show similar magnitudes and spatial gradients. The black line corresponding to the null anomalies crosses the same areas for both reanalysis. Also the spatial distributions of the wind impact maps for the two reanalyses are very similar (Figure 2c and d) and the same applies to the minimum/maximum values and significance level (black points). Both frequency time series of the NAO+ regime in winter for the two reanalyses are almost equals (Figure 2e and f). A similar close correspondence was observed for all WRs, wind speed and temperature impact maps and frequency diagrams obtained for both reanalysis datasets in all seasons.

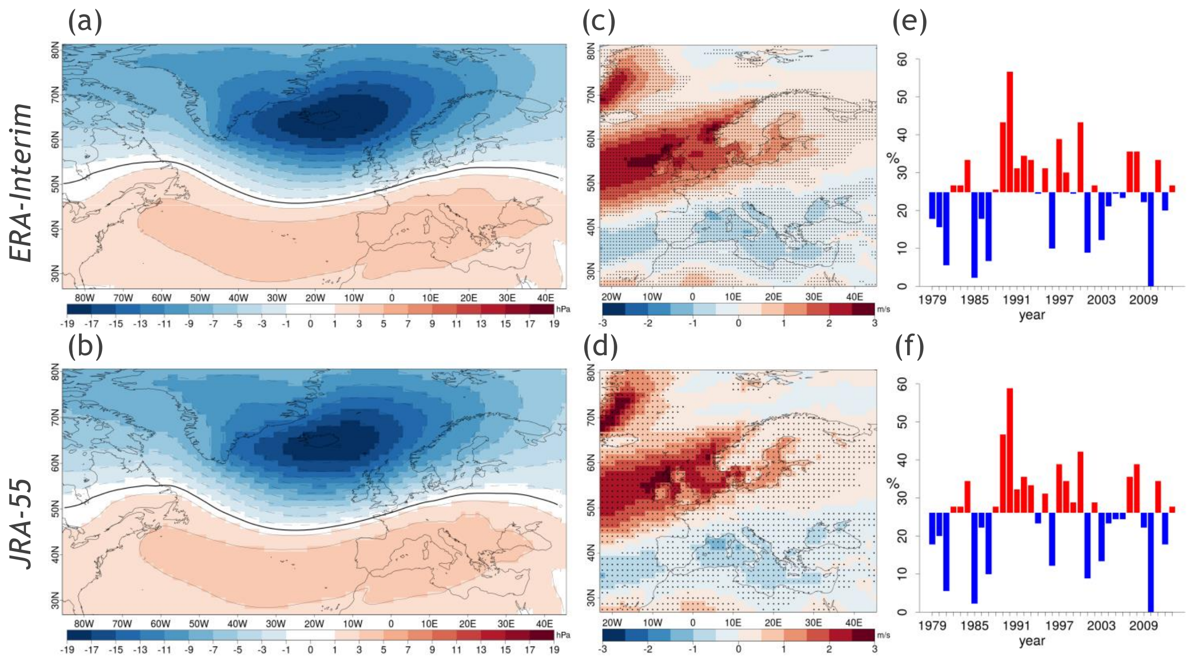

Figure 2. *WR comparison between ERA-Interim and JRA-55.*

(a) NAO+ regime for winter season (DJF) and period 1979-2013 obtained from the ERA-Interim reanalysis. Colours and contours indicate the average of SLP anomalies (in hPa) over all days associated to the NAO+ regime. (b) Same as (a) but for JRA-55 reanalysis. (c) Impact of the NAO+ regime on 10-m wind speed from ERA-Interim. Colours indicate the average wind speed anomalies (in m) of the days associated to the NAO+ regime. Black dots show grid points where the anomalies are significant at the 95% confidence level. (d) Same as (c) but for JRA-55. (e) ERA-Interim frequency time series (in %) of all days of the winter season belonging to the NAO+ regime. Red/blue bars show years with frequencies above/below the average of winter frequencies over 1979-2013. (f) Same as (e) but for the JRA-55 reanalysis.

For this reason, only results for the ERA-Interim dataset (the one with the highest resolution) are shown in this document, while results for JRA-55 dataset are illustrated in the catalogue[1].

3.2. Seasonal weather regimes and their impact on wind speed

For each WR, its spatial pattern and the impact on 10-m wind speed is shown in Figure 3 to Figure 6, with one figure per regime. These figures illustrate the seasonal evolution of the regime pattern and of its impact on wind speed. For example, the inter-seasonal evolution of the impact of WRs on wind speed is quite gradual in time; mean patterns weaken or strengthen, but without sudden changes of sign at a given site from one season to another, unless anomalies are already weak. Thus, the inter-seasonal impact variability is low for each WR.

3.2.1. NAO+ regime

The NAO+ regime is characterized by the reinforcement of the Icelandic low and the Azores high, resulting in an increased zonal flow of westerly winds towards central and northern Europe (Cassou et al., 2004). The strongest magnitude of the NAO+ regime anomalies is found in winter (Figure 3a) and spring (Figure 3b) followed by autumn (Figure 3c). The weakest magnitude is measured in summer (Figure 3d). The NAO+ negative SLP anomalies are slightly stronger than the positive ones in all seasons due to the lack of a latitudinal weighting of the SLP anomalies during the classification of the regimes. This observation is also valid for the other three regimes.

In winter, spring and autumn, the NAO+ regime has a highly positive and significant impact on wind speed in the north-western part of Europe (up to +3 m/s, equivalent to ~10 km/h) and a slightly negative and significant impact in the southern part (up to -1.5 m/s in winter). Thus, a clear spatial gradient is observed between northern and southern Europe (Figure 3e, 2f, 2g). The impact is stronger over water masses, especially where katabatic winds blow cold air from high-elevation areas into the open sea, such as along the western coast of Scotland and Norway. In general, England, Ireland and Denmark are the more affected European countries with a positive impact. In summer, the impact of the NAO+ regime on wind speed has a spatial distribution similar to the other seasons, but its magnitude is much lower, varying only between -0.5 m/s and +0.5 m/s for most of Europe (Figure 3h).

The climatological frequency of the NAO+ regime over the period 1979-2013 is 26.6% in autumn (Figure 3i), 24.8% in winter (Figure 3j), 18.7% in spring (Figure 3k) and 25.3% in summer (Figure 3l). The frequency time-series does not show any significant trend in any of the four seasons during this study period. Vrac et al. (2013) detected a negative and significant trend of the NAO+ regime during the winter months from December to February.

[1] http://www.bsc.es/ESS/catalogue

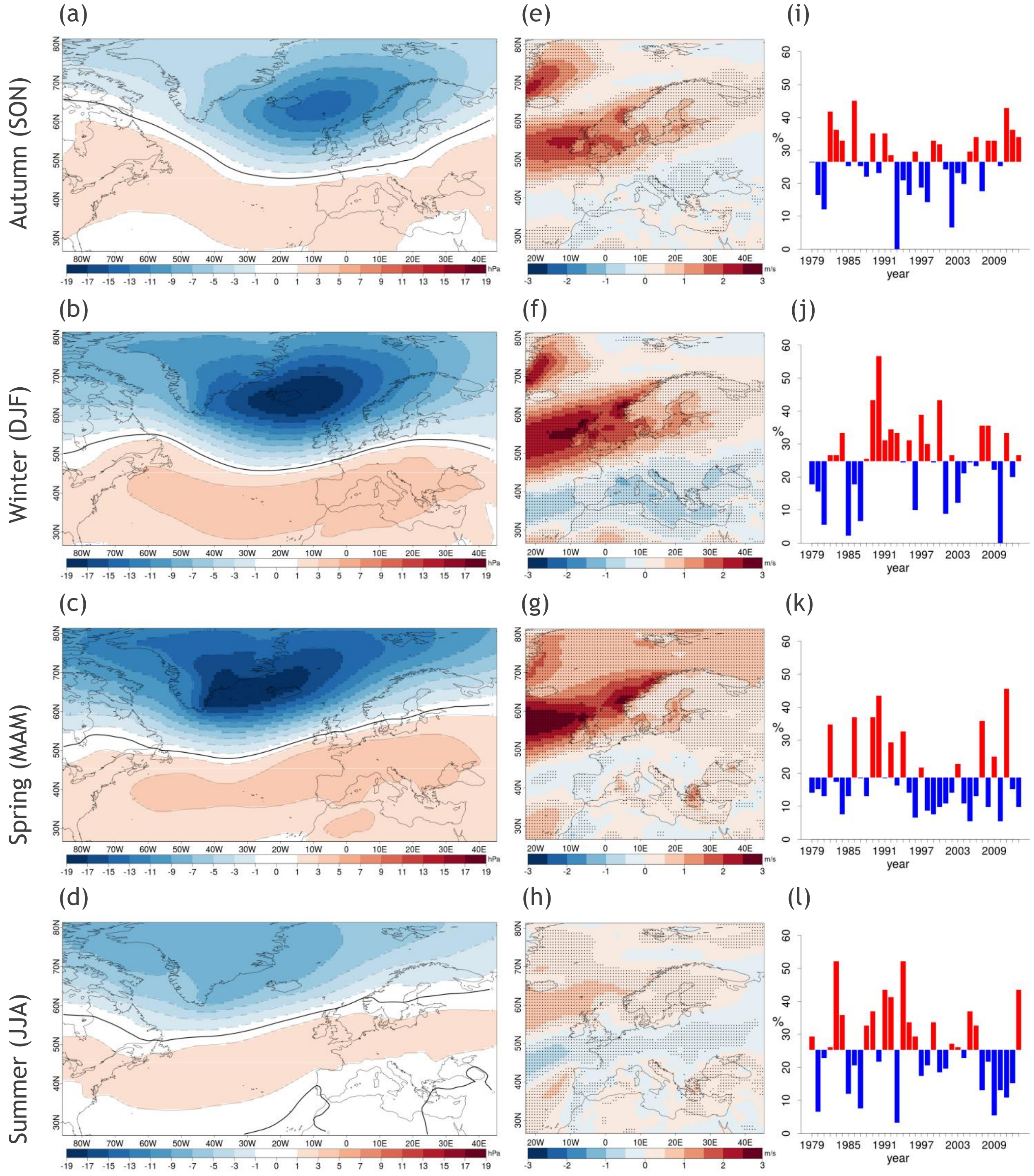

Figure 3. Seasonal evolution of the NAO+ weather regime in ERA-Interim over 1979-2013.

(a-d): Seasonal averages of SLP anomalies (in hPa) over all days associated with the NAO+ regime and the period. (e-h): Seasonal impact of the NAO+ regime on 10-m wind speed. Colors indicate the average of wind speed anomalies (in m/s) over the days associated with the NAO+ regime. Black dots show grid points where the anomalies are significant at the 95% confidence level. (i-l): frequency time series (in %) of the days belonging to the NAO+ regime. Red/blue bars show years with frequencies above/below the climatological frequency. From top to bottom, these patterns are shown for autumn (SON), winter (DJF), spring (MAM) and summer (JJA).

However, their analysis focused on a different period (1948-2011) and used geopotential height instead of SLP. Furthermore, in their case the raw data was filtered with a PCA and a different clustering method was chosen. A negative winter trend of NAO+ was found in this study when applying a PCA to the SLP data. The trend, however, was not statistically significant.

3.2.2. NAO- regime

The NAO- regime SLP anomalies are characterized by a spatial pattern similar to that of the NAO+ regime but with an opposite sign. The area with negative anomalies is centered over Azores and the area with positive anomalies is centered between Ireland and Greenland (Cassou et al., 2004). However, the patterns are not exactly symmetric. The absence of a SLP filter (such as a principal component analysis) before clustering allows to retain some small-scale features that otherwise would have been removed. The NAO- regime also shows a westward shift of the center of the positive regime anomalies from autumn to winter (Figure 4a to d).

The strongest magnitude of the NAO- regime anomalies is found in the winter (Figure 4a) and the weakest in the summer (Figure 4d). The areas where the impact of the NAO+ regime on wind speed is positive in Figure 3 are usually the areas where the impact of the NAO- regime is negative in Figure 4 and vice versa. The NAO- impact is highly negative (up to -3 m/s, equivalent to about -10 km/h) and significant in the northern part of Europe, especially in winter (Figure 4f) and slightly positive impact in the south-western part of Europe (up to +1.5 m/s near the Iberian Peninsula west coast). Eastern Europe is less affected during all seasons (Figure 4e, f, g and h). Both positive and negative impacts are stronger over the Atlantic Ocean than over the continental parts. In general, the Iberian Peninsula is the European region with the most positive impact. The amplitude of the regime anomalies decreases from winter to summer, and consequently, the strength of the impact also decreases. However, the position of the center of the regime anomalies does not change from winter to summer. So, the impact maps for the three seasons show a similar spatial pattern (albeit with decreasing magnitudes). Only in autumn, the different position of the center of the regime anomalies determines a different spatial pattern of the impact map.

The mean frequency of the NAO- regime is 26.2% in autumn (Figure 4i), 22.3% in winter (Figure 4j), 25.1% in spring (Figure 4k) and 21.7% in summer (Figure 4l). In summer, the Mann-Kendall test detected a positive and statistically significant trend at 95% confidence level (Figure 4l). It is particularly evident in the last years, when the frequencies are often above the 1979-2013 mean.

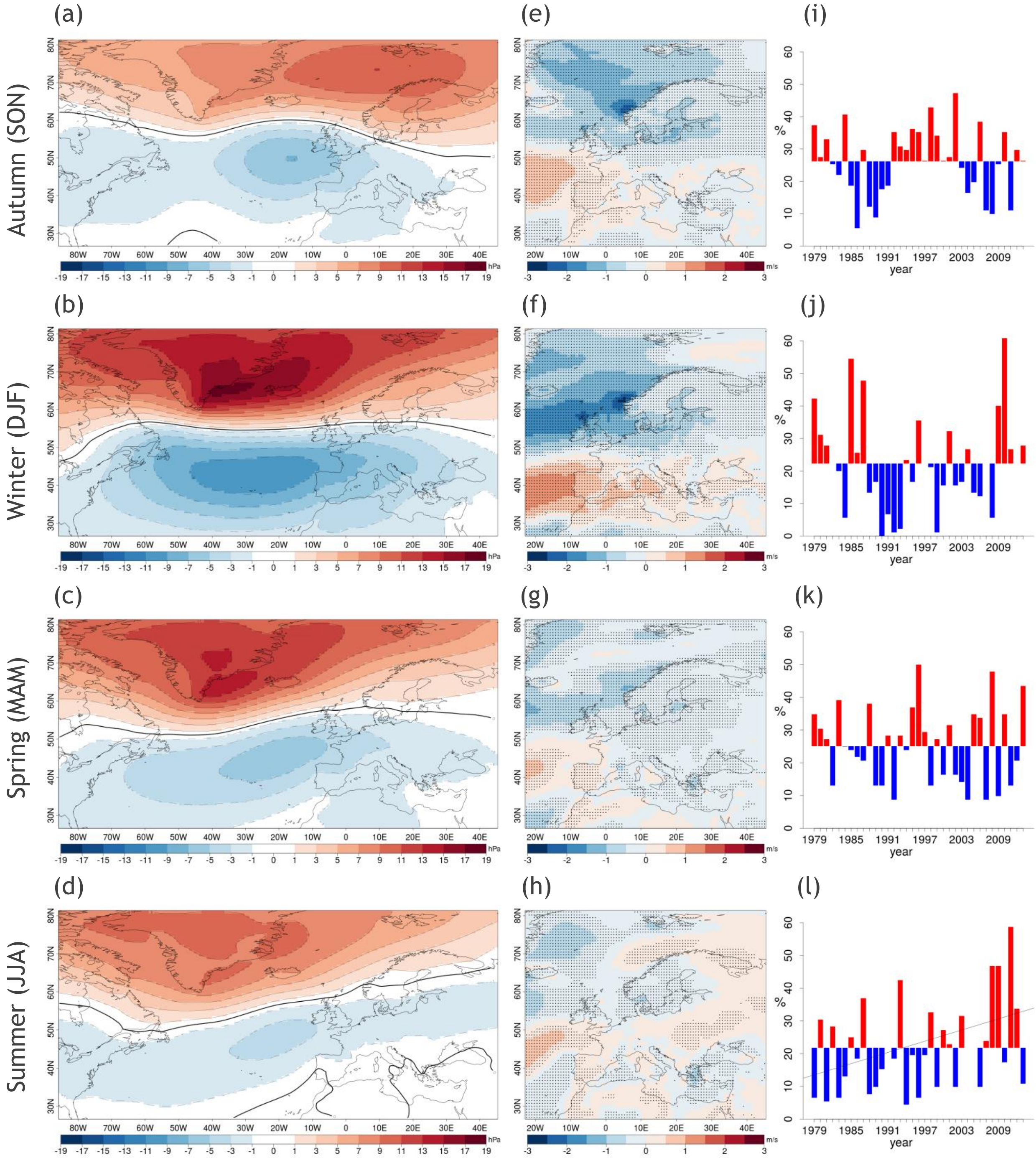

***Figure 4**. As Figure 3, but for the NAO- regime.*

3.2.3. Blocking regime

The Blocking regime (Figure 5) is characterized by positive anomalies centered over Scandinavia with negative anomalies over Greenland (Cassou et al., 2004). Its main effect is preventing the westerly flow of the jet-stream from reaching Europe by deviating northwestward instead (Barriopedro et al., 2006). The amplitude of the blocking regime anomalies is largest in winter, followed by autumn and weakest in summer.

As a consequence, the blocking regime has a highly negative and significant impact on wind speed in northern Europe and a slightly positive influence along the Mediterranean region (Figure 5e, f, g and h). The negative impact over Northern Europe is up to -2 m/s (equivalent to -7 km/h) in winter (Figure 5f), similar to the NAO- regime. Particularly in this season, it can have local positive and significant impacts due to the presence of katabatic winds, like the Bora in the Adriatic Sea (Paklar & Baji, 2005) and the Livas in the Ionian Sea (Zerefos C. et al., 2011).

The mean frequency of the blocking regime is 25.0% in autumn (Figure 5i), 28.2% in winter (Figure 5j), 31.4% in spring (Figure 5k) and 27.0% in summer (Figure 5l). It does not show any significant trend for any of the seasons.

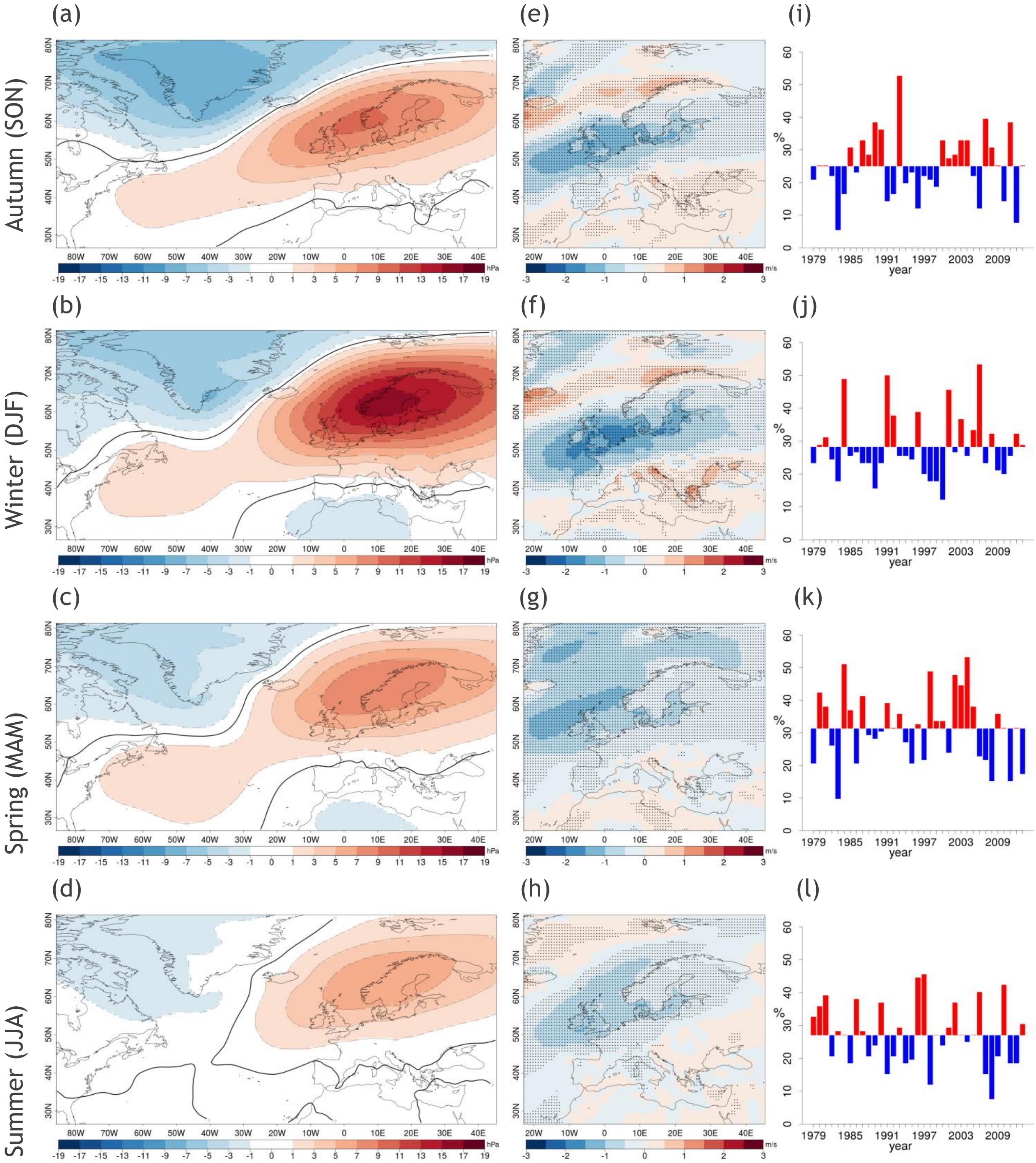

***Figure 5**. As Figure 3, but for the Blocking regime.*

3.2.4. Atlantic ridge regime

The Atlantic ridge regime (Figure 6) is characterized by strong positive SLP anomalies over the North Atlantic and negative anomalies over the Scandinavian region. The strongest dipole of pressure is found in autumn (Figure 6a), followed by winter (Figure 6b). In summer, this regime almost disappears because its positive anomalies are very weak and located over Greenland (Figure 6d).

The Atlantic ridge regime impact on wind speed is positive over central and northern Europe, up to 2.5 m/s in winter (Figure 6f). In this season, the positive impact of this regime can affect the Mistral katabatic wind over the Gulf of Lion as explained by Salameh et al. (2009). For all seasons, German, Poland and Denmark are the countries more affected by the increase of wind speed (Figure 6b). There is a negative impact over the western part of Europe, especially over Ireland and the Iberian Peninsula in autumn (Figure 6e).

The mean frequency of the Atlantic ridge regime is similar in all seasons: 22.3% in autumn (Figure 6e), 24.7% in winter (Figure 6f), 24.8% in spring (Figure 6g) and 25.9% in summer (Figure 6h). In spring, the frequency time series shows a positive and significant trend (Figure 6k). Compared to the others, the Atlantic ridge is also the regime showing the lowest inter-annual frequency variability, especially in autumn and spring.

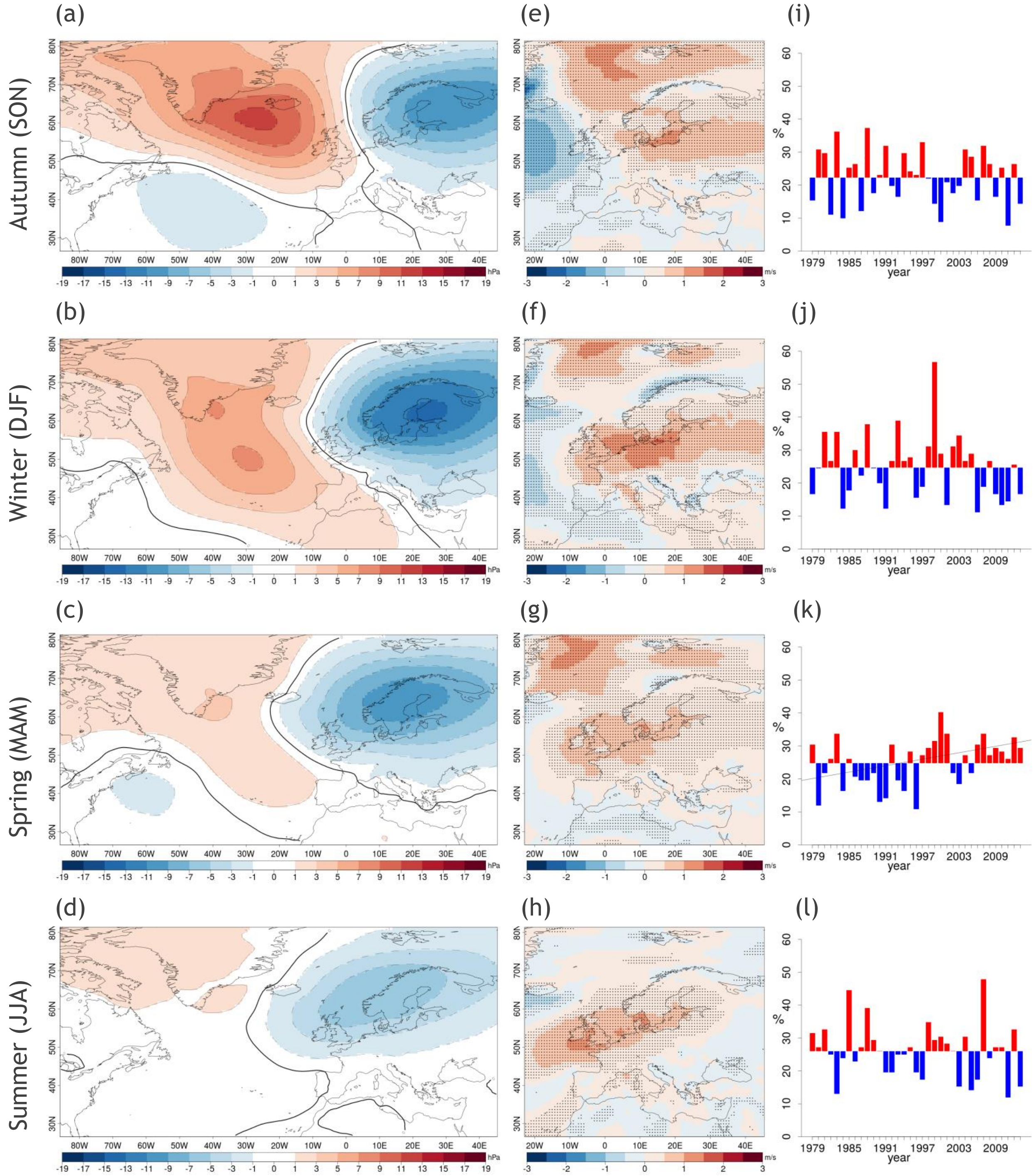

***Figure 6**. As Figure 3, but for the Atlantic Ridge regime.*

3.3. Seasonal weather regimes and their impact on temperature

The approach followed in the previous section was used in this one for describing the impact of each WR on the two-metre temperature field. The average of ERA-Interim temperature anomalies over the days associated with a given regime and season were obtained (Figure 7).

While the impact of the WRs on winds speed in Europe has not yet been object of study in the literature, the WR impact on temperature has already been studied by Fil & Dubus (2005) for the winter season (DJF) and by Cassou (2006) for summer season (JJA). In winter, the four impact maps in Figure 8 of Fil & Dubus (2005) are very close to those presented in Figure 7b-f-j-n of this study, even when different reanalysis, domains, periods and clustering algorithms were employed. This suggests a global spatial coherence of the impact of the WRs on temperature. In summer, the four impact maps of Cassou (2006) also show spatial patters mostly similar to those in Figure 7d-h-l-p but often with smaller magnitudes. This is because the authors omitted the days outside sequences of at least five consecutive days belonging to the same regime to increase the separation between WRs, which in turn increases the impact of the WRs on temperature.

3.3.1. NAO+ Regime

The NAO+ regime is characterized by the reinforcement of the Icelandic low and the Azores high, strengthening the storm track and the westerlies, which bring warm and wet air into northern Europe ((Fil & Dubus 2005). This behavior is confirmed in the impact map of the NAO+ regime during winter, which shows a strong positive and significant influence the regime on temperature, up to +4° C, in central and northern Europe (Figure 7b). However, in spring this regime seems to have a strong negative and significant influence all over Europe, especially in Eastern Europe (Figure 7c).

This apparent strong change of the impact sign from winter to spring is due to two factors: first, most of the NAO+ events in spring season (MAM) occur in March; and second, the March mean temperature is lower than the temperature of the rest of the spring. As a consequence, the average daily temperature anomalies for the NAO+ events in spring are mostly negative, since they reflect primarily March anomalies. This effect can be eliminated almost completely by analyzing the impact maps of the NAO+ regime on temperature at monthly time scale instead of seasonally (Figure 8). These monthly impact maps show positive anomalies over most of Europe for all three spring months.

During autumn (Figure 7a), a weak positive and significant impact around the Baltic Sea is observed and a weak negative impact elsewhere. The frequency of NAO+ regime doesn't change substantially during the three autumn months (SON). So, there doesn't appear to be any effect similar to the spring effect. During summer (Figure 7d), there is a weak positive influence everywhere in Europe, which is often significant. It is caused by the reduced amplitude of the regime anomalies.

3.3.2. NAO- Regime

The NAO- regime is characterized by negative SLP anomalies in southern Europe and positive anomalies over Iceland and Greenland. The impact of NAO- regime on temperature is almost symmetric to the impact of NAO+ (Figure 7e to h), except in spring, unless the monthly impact is considered (Figure 8) The highest NAO- impact on two-metre temperature is found in winter (Figure 7f), with strong negative and significant impact over northern Europe (up to -5° C) and a positive and significant impact along the Mediterranean basin. During the spring season, the negative impact decreases in magnitude and the positive impact remain constant in magnitude but it extends north, affecting also central Europe (Figure 7g). The other two seasons, summer and autumn, show a very weak impact, limited to ±1°C over the major part of Europe.

3.3.3. Blocking regime

The impact of this regime is strongly negative (up to +4° C) and significant over continental Europe in winter (Figure 7j) and a weaker positive and significant impact in spring with higher anomalies in Eastern Europe (Figure 7k). The other two seasons have even weaker anomalies (almost always within +/- 0.5° C). The autumn anomalies are negative almost all over Europe (Figure 7i), while the summer anomalies are negative only in the southern part and positive in the northern part (Figure 7l).

The spring impact of the blocking regime shows a globally positive impact over Europe but when studying the impact at monthly time scale, the positive impact disappears (results not shown). The blocking regime increases its frequency during the spring months. Therefore, more weight is given to the May temperature anomalies in its spring impact map, compared to the same effect described in the NAO+ regime section. The other two regimes are also affected since the frequency of a WR in May is always different from that in March but to a lesser degree.

3.3.4. Atlantic ridge regime

This regime brings cold air from Greenland to the north-western part of Europe, so its impact on temperature is mostly negative in western Europe in all seasons while it is positive over eastern Europe in all seasons (Figure 7m, 8n, 8o, 8p), particularly in winter (up to +4° C). It's in this season (Figure 7n) in fact when a clear east-west gradient of temperature anomalies is observed. The other three seasons show weaker positive anomalies, especially in spring (Figure 7o) and summer (Figure 7p). Overall, for each season the spatial impact of this regime on temperature is roughly the opposite of the impact of the blocking regime.

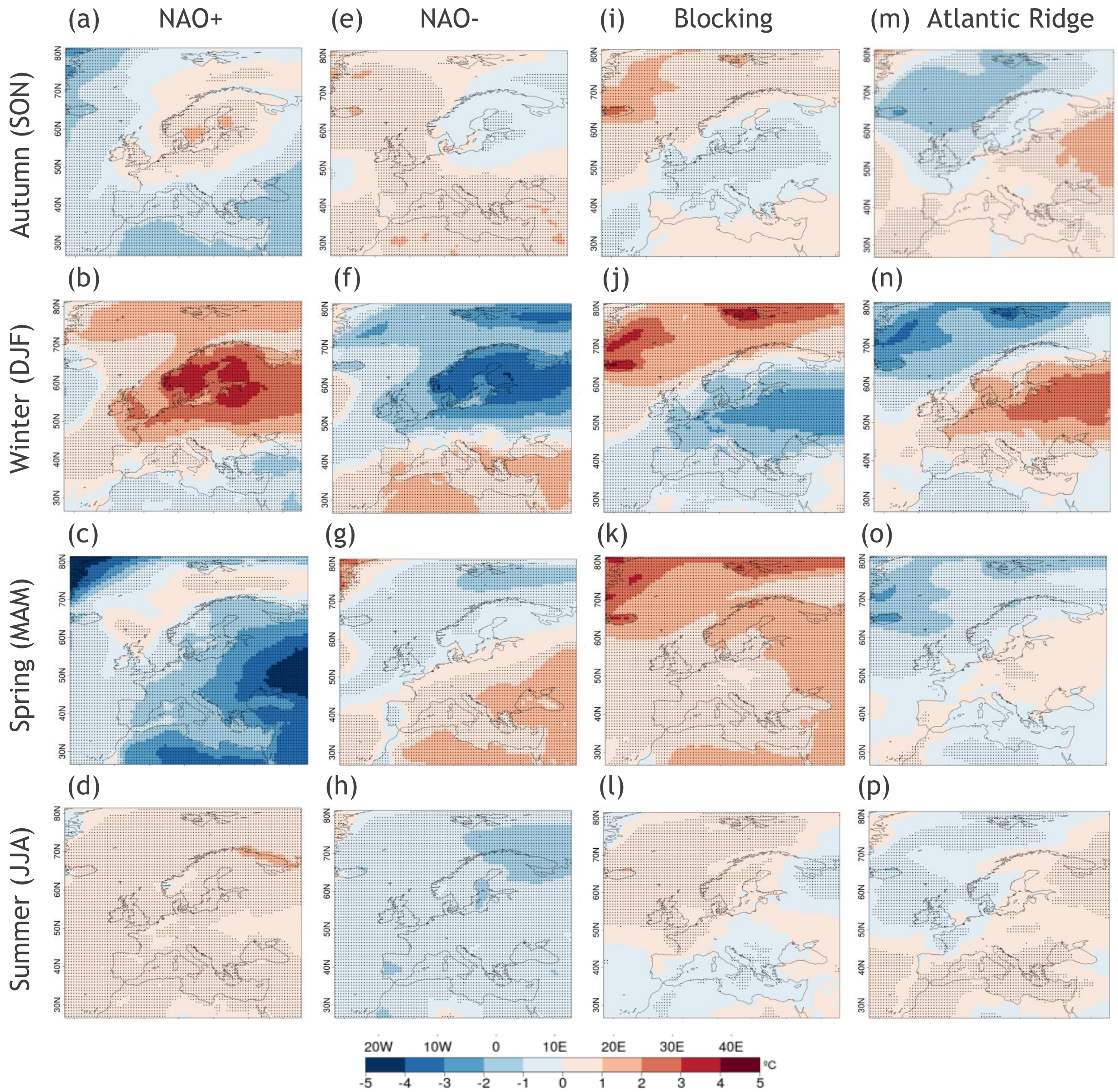

***Figure 7**. Seasonal evolution of the impact of WRs on 2-m temperature.*

(a-p): Seasonal evolution of the impact of the four WRs on 2-m temperature from autumn (SON, top row) to summer (JJA, bottom row). Colors indicate the average of ERA-Interim 2-m temperature anomalies (in °C) over the days associated to the corresponding regime and the period 1979-2013. Black dots show grid points where the anomalies are significant at the 95% confidence level for a t-test.

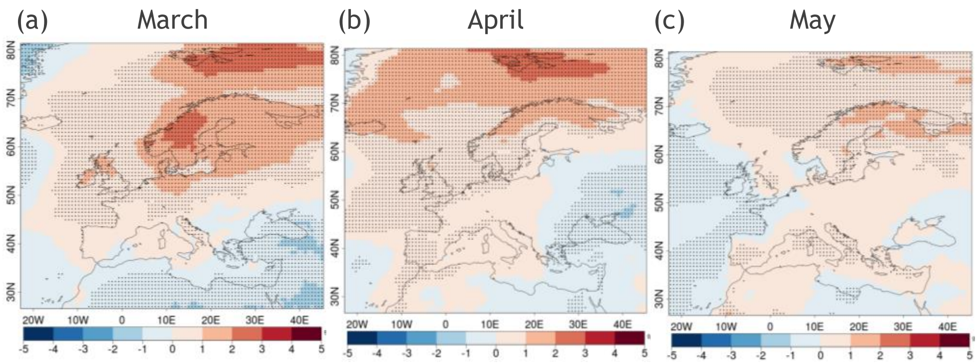

Figure 8*. Monthly impact of NAO+ regime on temperature during spring.*

Monthly evolution from March (a) to May (c) of the impact of NAO+ regime on 2-m temperature. Colours indicate the average of ERA-Interim 2-m temperature anomalies (in °C) over the days associated to the NAO+ regime and the period 1979-2013. Black dots show grid points where the anomalies are significant at the 95% confidence for a t-test.

4. Conclusions

The main aim of this work was to analyze the mechanisms driving wind speed and temperature seasonal variability over Europe using the weather regime paradigm, to define a set of reference WRs that will be applied to validate seasonal forecast systems.

To this end, the four North Atlantic-European weather regimes (NAO+, NAO-, blocking and Atlantic ridge) were used to classify the daily SLP data using clustering analysis. The classification was used to evaluate the impact on the average wind speed and temperature anomalies of each regime. We showed that weather regimes are a useful conceptual model to understand the variability of both wind speed and temperature in Europe as they can have a large impact on day-to-day variations of these variables, not only in winter but also during the other seasons of the year. To the best of our knowledge, results for spring and autumn in the North-Atlantic region have not been published elsewhere.

Particularly important is the correspondence found for all the results of the two reanalysis employed, ERA-Interim and JRA-55. It demonstrates that changing the observational source has little or no influence on the impact of the WRs on both wind speed and temperature. Thus, it is possible to select the dataset with the higher resolution (ERA-Interim) as reference dataset. Results for JRA-55 are shown in the catalogue[2].

Even if the impact of the WRs on both wind speed and temperature is often significant, its range for wind speed is limited to ±3 m/s above/below the wind speed seasonal climatology (roughly equivalent to ±11 km/h), while the impact on temperature varies within a range of ±5° C. The impact on temperature is more spatially homogeneous than the impact on wind speed, because it does not show any circumscribed area with opposing impact sign than the nearby regions. This is probably due to the temperature's higher coherence.

In winter, which is the season with the highest amplitudes of the regime anomalies, the impact of the NAO+ regime on wind speed and temperature shows a strong longitudinal gradient. It is positive and significant in large parts of northern Europe for both variables. The NAO- impact follows a mirror image of the NAO+, with inverted gradients and anomalies. The spatial distribution of the impact of the blocking regime on wind speed is quite similar to that of the NAO- regime, while the impact on temperature is negative and significant all over Europe. The Atlantic ridge regime has a positive and significant effect in most of Europe on both wind speed and temperature. In general, the impact of WRs on wind speed and temperature is stronger in winter and weaker in summer. The other seasons show an intermediate behavior. Impact on wind speed is often stronger over oceans than over land masses, probably related to the high climatological wind speed values obtained over water masses due to the reduced friction.

A critical factor individuated was the strong dependence of the impact on temperature on the

[2] http://www.bsc.es/ESS/catalogue

climatological period employed for computing seasonal anomalies. In particular, spring and autumn impacts are quite sensible to a change in the frequency of occurrence of the WRs. For this reason, we recommend to measure spring and autumn impact using monthly anomalies instead of seasonal ones.

5. Acknowledgements

The authors acknowledge funding support from the RESILIENCE (CGL2013-41055-R) project, funded by the Spanish Ministerio de Economía y Competitividad (MINECO). We are also grateful to Dr. Christian Viel of Météo France for the helpful discussions regarding this work.

6. References

Barriopedro, D. et al., 2006. A climatology of Northern Hemisphere blocking. *Journal of Climate*, 19(6), pp.1042–1063.

Cassou, C. et al., 2004. North Atlantic winter climate regimes: Spatial asymmetry, stationarity with time, and oceanic forcing. *Journal of Climate*, 17(5), pp.1055–1068.

Cassou, C., Terray, L. & Phillips, A., 2006. Weather Regimes and European heat waves 2003 a case study. *JPL OSE Meeting*, pp.35–42.

Cassou, C., Terray, L. & Phillips, A.S., 2005. Tropical Atlantic influence on European heat waves. *Journal of Climate*, 18(15), pp.2805–2811.

Cattiaux, J. et al., 2013. North-Atlantic dynamics and European temperature extremes in the IPSL model: Sensitivity to atmospheric resolution. *Climate Dynamics*, 40(9-10), pp.2293–2310.

Couto, A. et al., 2015. Impact of Weather Regimes on the Wind Power Ramp Forecast in Portugal. *IEEE Transactions on Sustainable Energy*, 6(3), pp.934–942.

Dee, D.P. et al., 2011. The ERA-Interim reanalysis: Configuration and performance of the data assimilation system. *Quarterly Journal of the Royal Meteorological Society*, 137(656), pp.553–597.

Ferranti, L., Corti, S. & Janousek, M., 2015. Flow-dependent verification of the ECMWF ensemble over the Euro-Atlantic sector. *Quarterly Journal of the Royal Meteorological Society*, 141(688), pp.916–924.

Fil, C. & Dubus, L., 2005. Winter climate regimes over the North Atlantic and European region in ERA40 reanalysis and DEMETER seasonal hindcasts. *Tellus, Series A: Dynamic Meteorology and Oceanography*, 57(3), pp.290–307.

Hafez, Y.Y. & Almazroui, M., 2014. Recent Study of Anomaly of Global Annual Geopotential Height and Global Warming. *Atmospheric and Climate Sciences*, 4, 347-357(July), pp.347–357.

Hartingan, J.. & Wong, M.., 1979. Algorithm AS 136 A K-Means Clustering Algorithm. *Journal of the Royal Statistical Society*, 28(1), pp.100–108.

Hurrell, J.W. & Deser, C., 2009. North Atlantic climate variability: The role of the North Atlantic Oscillation. *Journal of Marine Systems*, 78(1), pp.28–41.

Johnson, N.C., Feldstein, S.B. & Tremblay, B., 2008. The continuum of northern hemisphere teleconnection patterns and a description of the NAO shift with the use of self-organizing maps. *Journal of Climate*, 21(23), pp.6354–6371.

Kobayashi, S. et al., 2015. The JRA-55 Reanalysis: General Specifications and Basic Characteristics. *Journal of the Meteorological Society of Japan. Ser. II*, 93(1), pp.5–48.

Michelangeli, P.-A., Vautard, R. & Legras, B., 1995. Weather Regimes: Recurrence and Quasi Stationarity. *Journal of the Atmospheric Sciences*, 52(8), pp.1237–1256.

Neal, R. et al., 2016. A flexible approach to defining weather regimes and their application in weather forecasting over Europe. *Meteorological Applications*, 1, pp.1–12.

Paklar, G.B. & Baji, A., 2005. Annales Geophysicae Bora-induced currents corresponding to different synoptic conditions above the Adriatic. *Annales Geophysicae*, 23(1988), pp.1083–1091.

Salameh, T. et al., 2009. Statistical downscaling of near-surface wind over complex terrain in southern France. *Meteorology and Atmospheric Physics*, 103(1-4), pp.253–265.

Trigo, R.M. et al., 2004. North Atlantic oscillation influence on precipitation, river flow and water resources in the Iberian Peninsula. *International Journal of Climatology*, 24(8), pp.925–944.

Vrac, M., Vaittinada Ayar, P. & Yiou, P., 2014. Trends and variability of seasonal weather regimes. *International Journal of Climatology*, 34(2), pp.472–480.

Yiou, P. & Nogaj, M., 2004. Extreme climatic events and weather regimes over the North Atlantic: When and where? *Geophysical Research Letters*, 31(7), pp.1–4.

Zerefos C. et al., 2011. Environmental, Economic and Social Impacts of Climate Change in Greece B. of Greece, ed. *Bank of Greece*, p.494.